Journal of Japan Association for Earthquake Engineering, Vol. 26, No. 3, 2026
[Technical Report (Translated Paper)]

PRACTICAL APPLICATION OF PROBABILISTIC FAULT DISPLACEMENT HAZARD ANALYSIS BASED ON DISTANCE FROM THE EARTHQUAKE SOURCE FAULT

Naoki NISHIZAKA[1, 2], Kozo ONISHI[3], Yoshihiko ISHIKAWA[4], Hiromichi YANO[5], Jun'ichi MIYAKOSHI[6], Michiharu IKEDA[7] and Takeshi TSUJI[8]

[1] Member, Dr. Eng., Shikoku Electric Power Co., Inc., Kagawa, Japan, nishizaka14981@yonden.co.jp
[2] School of Engineering, University of Tokyo
[3] Member, Dr. Sc., Shikoku Electric Power Co., Inc., Kagawa, Japan, oonishi16286@yonden.co.jp
[4] M. Eng., Shikoku Electric Power Co., Inc., Kagawa, Japan, ishikawa15596@yonden.co.jp
[5] M. Sc., Shikoku Electric Power Co., Inc., Kagawa, Japan, yano17507@yonden.co.jp
[6] Member, Dr. Eng., Ohsaki Research Institute, Inc., Tokyo, Japan, miya@ohsaki.co.jp
[7] Dr. Sc., Shikoku Research Institute, Inc., Kagawa, Japan, m-ikeda@ssken.co.jp
[8] Dr. Sc., Professor, School of Engineering, University of Tokyo, Tokyo, Japan, tsuji@sys.t.u-tokyo.ac.jp

ABSTRACT: Fault displacements can cause structural damage and loss of functionality. The conventional framework for probabilistic fault displacement hazard analysis (PFDHA) estimates the characteristics of distributed ruptures as a function of distance from the principal fault. Recently, revised fault displacement prediction equations (FDPEs) have been proposed as a means to capture the attenuation characteristics of fault displacement in the far-field as a function of distance from the subsurface earthquake source faults, without classifying surface ruptures as principal or distributed. These FDPEs enable us to address many of the challenges identified during the first practical application of PFDHA in Japan, which was conducted at the Ikata site in northwestern Shikoku. In this study, we conducted a case study of PFDHA based on distance from the earthquake source faults at the Ikata site. Based on the results, we report the characteristics of the new FDPEs and insights gained from their practical application at the Ikata site.

Keywords: *Probabilistic fault displacement hazard analysis, Median Tectonic Line active fault zone, Earthquake source fault*

1. INTRODUCTION

When large fault displacements occur directly beneath structures during an earthquake, the structures may sustain damage and lose their functionality. Strict regulations on the siting of nuclear facilities have been established regarding fault displacements. Probabilistic Fault Displacement Hazard Analysis (PFDHA) is recommended in the safety guide established by the International Atomic Energy Agency

(IAEA) when fault displacement may affect the foundations of safety-critical facilities[1)–3)]. In recent years, PFDHA has been increasingly applied to the siting and design of many types of crucial infrastructure, such as dams and pipelines[4), 5)]. The conventional framework for PFDHA classifies surface ruptures as either principal (closely related to the earthquake source faults) or distributed (occurring secondarily or as a subsidiary rupture caused by the activities of the principal fault). For facilities located so as to avoid the immediate vicinity of the principal fault, fault displacement prediction equations (FDPEs), consisting of an equation for surface rupture probability and an equation for the amount of fault displacement, have been proposed to calculate the conditional probability of surface ruptures at a specific site location for distributed ruptures and the conditional probability of exceedance on the distributed ruptures, based on distance from the principal fault[1), 6)–11)]. Japan contains numerous faults as a result of its geological setting, and thus is earthquake-prone. The first full-scale PFDHA in Japan targeting a specific structure was implemented at the Ikata site in northwestern Shikoku (Nishizaka et al.[12)]). This application utilized the seismic source characterization model for the Ikata site (Kumamoto et al.[13)]), for which an advanced probabilistic seismic hazard analysis model was constructed through Japan's first Senior Seismic Hazard Analysis Committee (hereafter SSHAC) Level 3 project. Part of this work was an examination of concrete challenges in applying PFDHA at the practical level. Note that in the present study, which makes extensive use of logic trees for the practical implementation of PFDHA at an actual site, the entire logic tree combining the seismic source characterization model and the fault displacement characterization model is referred to as the PFDHA model.

In the Iyo-nada Sea offshore of the Ikata site, the principal fault is the Iyo-nada Segment of the Median Tectonic Line active fault zone (MTLAFZ), which exhibits dominant right-lateral strike slip; this fault segment is thought to reach the deep-seated earthquake source fault by cutting sedimentary layers nearly vertically approximately 8 km offshore. Although the segment is accompanied by distributed faults to its south (approximately 6–8 km offshore from the Ikata site), no active faults have been recognized within approximately 6 km of the site (Fig. 1). According to PFDHA results for the Ikata site[12)], the effects of characteristic earthquakes associated with activity on the Iyo-nada Segment dominate the fault displacement hazard. The annual frequency of fault displacements occurring directly beneath critical seismic-resistant facilities was approximately 1×10^{-7}. Furthermore, many challenges were identified through the implementation of PFDHA. Beyond the fundamental methodological challenge that epistemic uncertainty when classifying surface ruptures as principal or distributed markedly impacts the development of FDPEs, other challenges include expanding surface rupture data to areas far from the principal fault, developing FDPEs that can account for the presence or absence of pre-existing active faults, and establishing a methodology that can consider site-specific seismotectonics.

To capture the attenuation characteristics of fault displacements at distances far from the earthquake source faults, new FDPEs for strike-slip faults have been proposed (Nishizaka et al.[16)]). These equations revised the conventional FDPEs by adopting the distance from the subsurface earthquake source faults, without classifying surface ruptures as principal or distributed. These revised FDPEs introduced a new term related to the distance from the mapped, pre-existing active faults to account for the potential reactivation of pre-existing active faults. The FDPEs were developed using individual datasets of robust and extensive surface rupture data associated with the 2016 Kumamoto and the 2019 Ridgecrest earthquakes, obtained through remote sensing techniques (Nurminen et al.[17)]). Therefore, applying the FDPEs developed from the surface rupture data associated with the 2016 Kumamoto earthquake, specifically the dataset from the outer zone of southwestern Japan that shares common seismotectonics with the Ikata site, provides a foundation to address many of the challenges identified from the previous PFDHA practice at the Ikata site. In the present study, we incorporated these newly proposed FDPEs[16)], which are based on distance from the strike-slip earthquake source faults, into the PFDHA model for the Ikata site. We compared the new results with previously reported PFDHA results for the site[12)], and herein report on the characteristics of the new FDPEs and the insights gained from their application at the Ikata site.

2. ANALYSIS MODELS

According to the previous PFDHA practice at the Ikata site[12)], the impact of characteristic earthquakes dominates the fault displacement hazard, whereas the impact of earthquakes smaller than characteristic magnitude is minor. Therefore, in this study we considered characteristic earthquakes occurring on the MTLAFZ (Iyo-nada Segment) as the target seismic source. The framework of the PFDHA model consists of a seismic source characterization model and a fault displacement characterization model. For the former, the seismic source characterization model for the Ikata site[13)], based on the SSHAC Level 3 Guidelines and identical to that in the previous study[12)], was adopted without any modification. For the latter, in contrast, to understand the characteristics of the new FDPEs[16)] based on distance from the earthquake source faults, we followed the logic tree constructed in the previous study[12)] and added a branch for the new FDPEs. Details of the seismic source characterization model have been described in previous studies[12)–14)], and only an outline is provided herein.

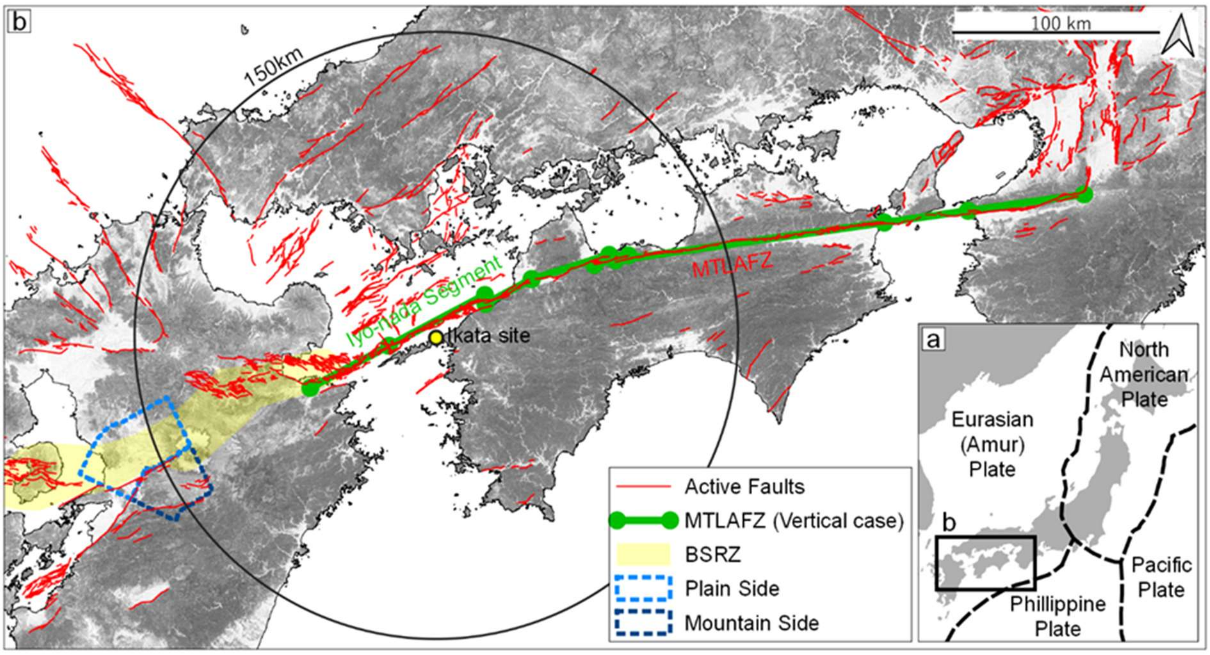

Fig. 1 Distribution of active faults around the Ikata site and segmentation of the Median Tectonic Line active fault zone (MTLAFZ). Active fault distribution and segmentation are based on the Ikata SSHAC Project Final Report[14)]. The yellow shaded area corresponds to the Beppu–Shimabara Rift Zone (BSRZ; Kusumoto[15)]). The light blue and dark blue dashed outlines indicate the area of the analysis grid on the plain and mountain sides, respectively, for the 2016 Kumamoto earthquake according to Nishizaka et al.[16)].

2.1 Seismic source characterization model

Characteristic earthquakes occurring on the Iyo-nada Segment are earthquakes with a specific earthquake source fault plane. The seismic source characterization model (logic tree) that specifies earthquake location and geometry and sets their magnitude and earthquake probability of occurrence (Fig. 2) was developed through the Ikata SSHAC Project[13), 14)]. The evaluation items for the earthquake location and geometry are the planar position and the fault width, which together are characterized in terms of the fault dip angle and the shortest distance from the fault. The evaluation items for earthquake magnitude are the selection of magnitude prediction equations. The evaluation items for the earthquake probability of occurrence are the mean recurrence interval, the time-dependent or time-independent occurrence model (Brownian Passage Time [BPT] distribution or Poisson process), the elapsed time since the latest faulting event, the aperiodicity parameter, and the methodology for evaluating seismic linkage. Within the PFDHA framework, earthquake location (shortest distance from the fault) and magnitude are related to the surface rupture probability and the probability of exceedance on the surface ruptures. Multiplying the three parameters in the fault displacement characterization model (described later) by the earthquake probability of occurrence in the seismic source characterization model allows determination of the annual frequency at which the fault displacement on the ground surface exceeds a specified amount at a given site (i.e., the annual exceedance frequency [AEF]).

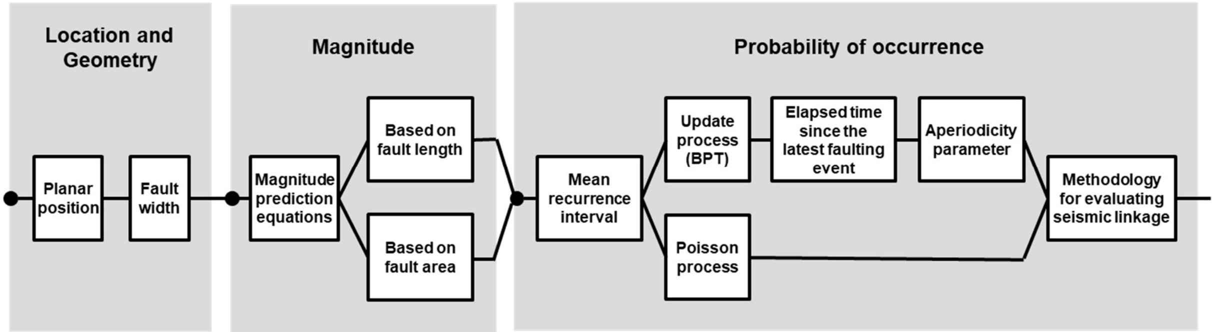

Fig. 2 Overview of the seismic source characterization model (logic tree)

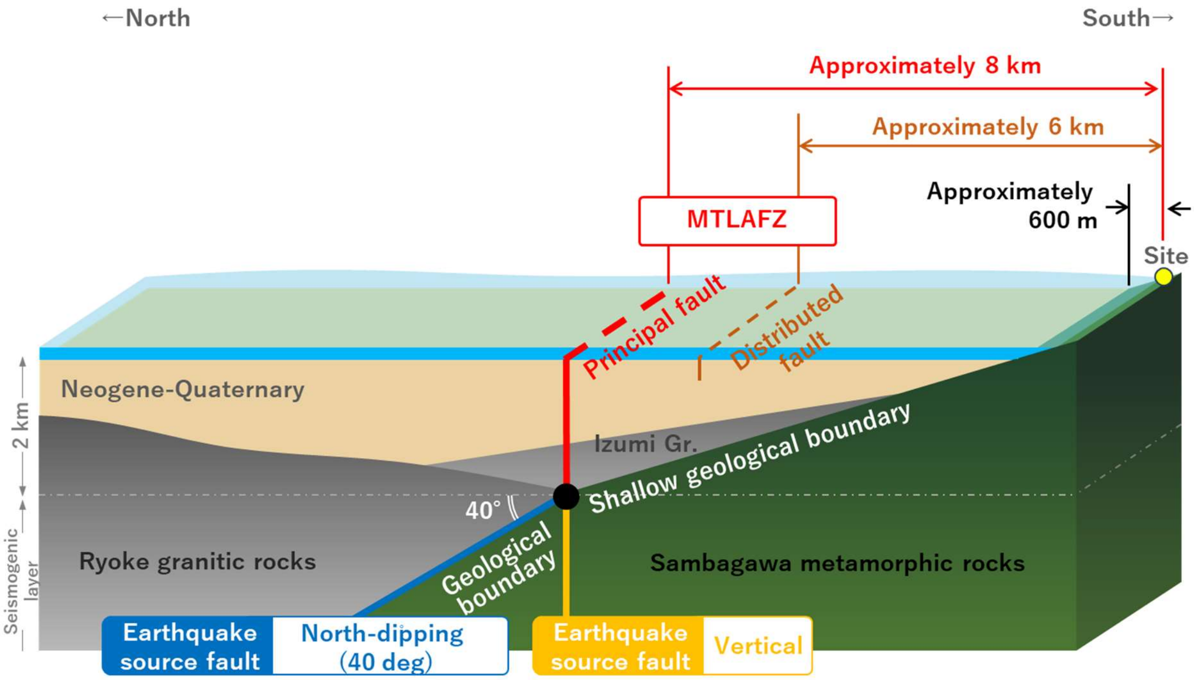

Fig. 3 Epistemic uncertainties on the dip angle of the Iyo-nada Segment. MTLAFZ, Median Tectonic Line active fault zone.

The Ikata SSHAC Project conducted comprehensive data collection and vigorous discussions regarding the fault dip angle and the shortest distance from the principal fault of the MTLAFZ (Iyo-nada Segment) passing north of the Ikata site, modeling their epistemic uncertainties (Figs. 3 and 4). For the dip angle of the earthquake source fault located at > 2 km depth, two branches were defined: "Vertical (90°)" as a representative value for nearly vertical fault planes, which are common in strike-slip faults, and "North dip (40°)" as the representative value for the north-dipping geological boundary of the Median Tectonic Line at depths equivalent to the seismogenic layer. Because the overall distribution of experts' opinions meant that both scenarios were considered equally plausible, equal weights (0.5:0.5) were assigned to each of these branches (Fig. 4). However, for the fault dip angle at shallower depths, the "Vertical (90°)" branch was set for both the "Vertical (90°)" earthquake source fault and the "North dip (40°)" earthquake source fault, such that the principal fault of the Iyo-nada segment is interpreted to pass approximately 8 km offshore. In addition, based on the view that the coastal geological boundary of the Median Tectonic Line in the shallow section (passing approximately 600 m offshore from the Ikata site) represents active faults, a branch of "North dip (low angle)" was added to the "North dip (40°)" branch. Although there are no data to support activity on such a low-angled geological boundary, some opinions suggest that it may be a possibility. Considering that the possibility of low-angle strike-slip movement cannot be completely ruled out if the fault strength and friction coefficient are markedly small, a weight of 0.1 was assigned to the "North dip (low-angle)" branch to represent the edge of the range[14]. Takahashi et al.[18] showed through marine seismic profiles that no activity can be recognized after the Quaternary Period on the shallow geological boundary. This geological boundary in the shallow section is not an active fault and does not represent a "capable fault" as defined in the IAEA Safety Guide[2]. Furthermore, regardless of the setting of the fault dip angle, the three-dimensional shortest distance from the subsurface earthquake source faults is approximately 8 km, and the surface shortest distance from the mapped, pre-existing active faults is approximately 6 km.

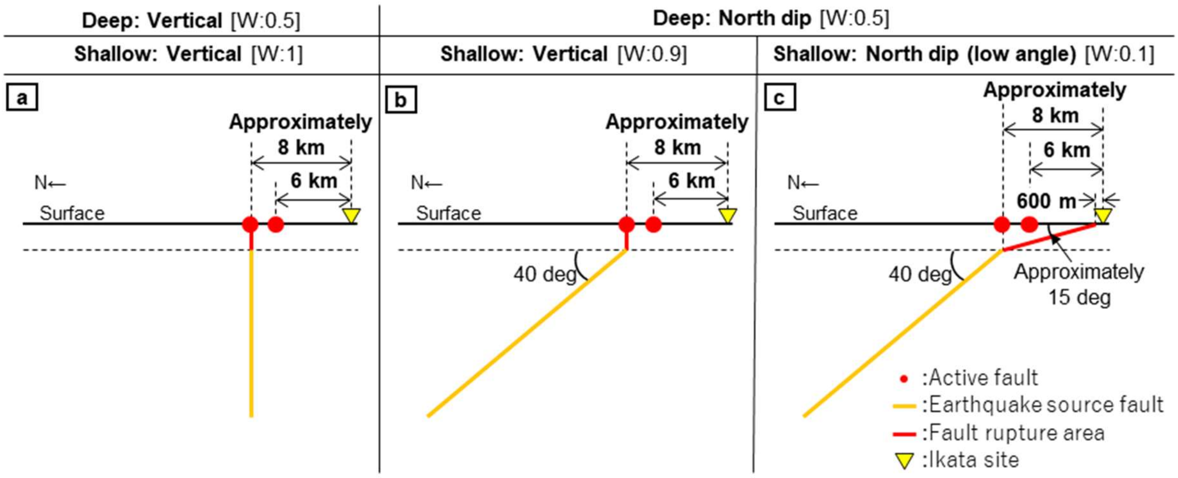

Fig. 4 Weight settings for the fault dip angles and the shortest distances to faults in the Iyo-nada Segment. W, weight.

2.2 Fault displacement characterization model

The fault displacement characterization model (logic tree) for characteristic earthquakes occurring on the Iyo-nada Segment consists of two branches to select FDPEs for calculating the conditional probability of surface ruptures and the conditional probability of exceedance on the distributed ruptures at the Ikata site. One branch adopts the conventional FDPEs based on distance from the principal fault; the other adopts the newly proposed FDPEs based on distance from the earthquake source faults (Fig. 5). Because the latter FDPEs were developed using a dataset from the outer zone of southwestern Japan, which shares common seismotectonics with the Ikata site, it was given greater weight. The weights for the conventional and new FDPEs were set to 0.3:0.7 to ensure that the characteristics of the new FDPEs are clearly reflected in the median hazard curve.

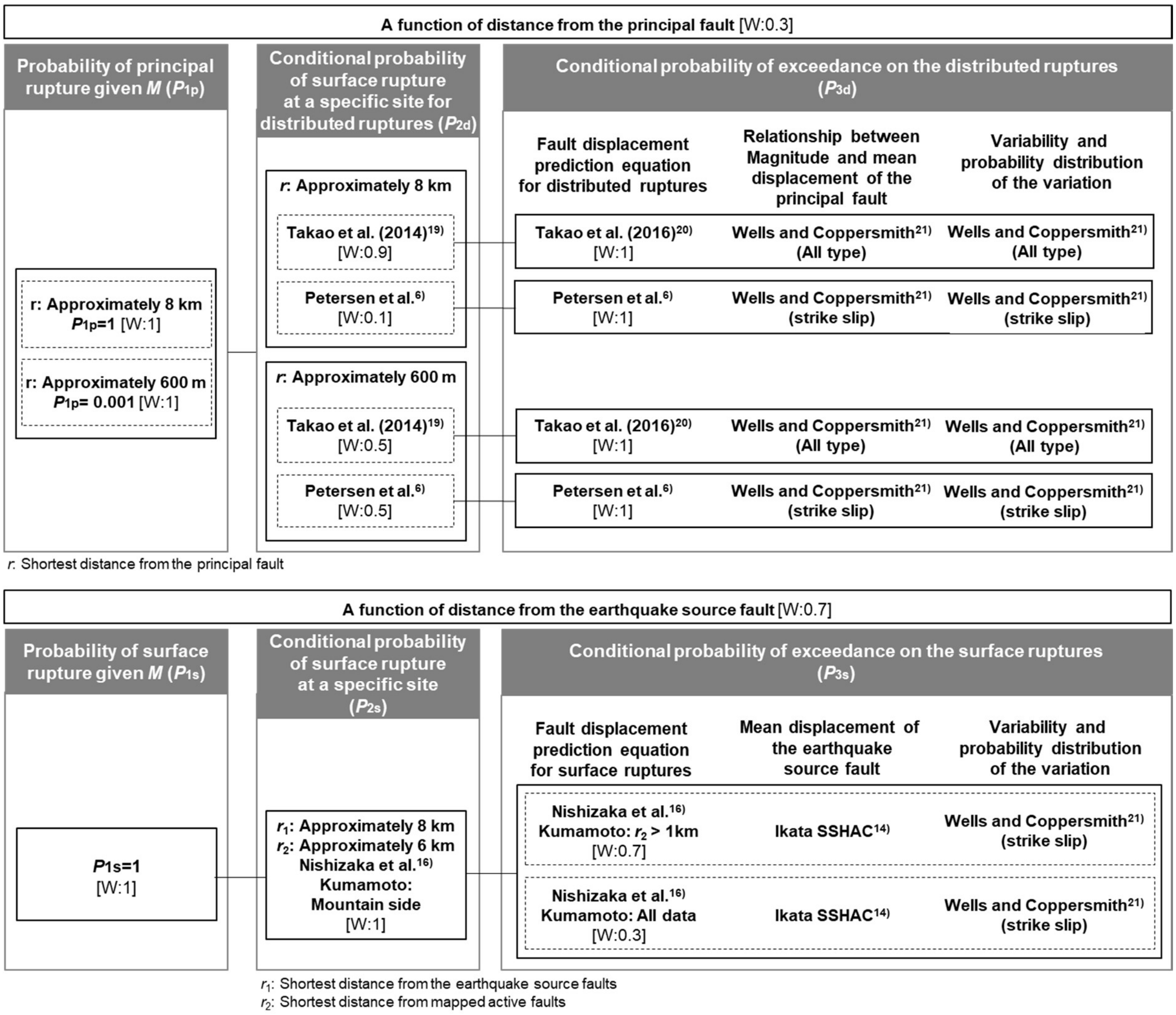

Fig. 5 Fault displacement characterization model (logic tree). W, weight.

The logic tree for the FDPEs based on distance from the principal fault consists of the probability of principal rupture given a magnitude M (P_{1p}), the conditional probability of surface rupture at a specific site location for distributed ruptures (P_{2d}), and the conditional probability of exceedance on the distributed ruptures (P_{3d}). We followed the logic tree constructed in the previous study[12]. The probability of principal rupture given a magnitude M (P_{1p}) assumes that the principal fault will always rupture the surface ($P_{1p} = 1$) when the shortest distance from the principal fault is approximately 8 km (i.e., when the principal fault is vertical at < 2 km depth) (Figs. 4(a), (b)). For the shortest distance of approximately 600 m from the principal fault (when the geological boundary in the shallow part is interpreted as the principal fault; Fig. 4(c)), $P_{1p} = 0.001$. To calculate the conditional probability of surface rupture at a specific site location for distributed ruptures (P_{2d}), we adopted the FDPEs of Takao et al. (2014)[19] and Petersen et al.[6]. After calculating the FDPE using unit cell sizes of 250 m x 250 m for the former and 200 m x 200 m for the latter, we calibrated the results with an area ratio equivalent to the value for 160 m x 160 m, which corresponds to the area of critical seismic-resistant facilities at the Ikata site, following the method given by the U.S. Nuclear Regulatory Commission[22]. Regarding the weight settings for the FDPE by Takao et al. (2014)[19] and Petersen et al.[6], the weight was set to 0.9:0.1 when the shortest distance from the principal fault was approximately 8 km, and to 0.5:0.5 when the shortest distance from the principal fault was approximately 600 m. The conditional probability of exceedance on the distributed ruptures (P_{3d}) was calculated using the FDPEs of Takao et al. (2016)[20] and Petersen et al.[6] respectively, to maintain consistency with the calculation of the conditional probability of surface rupture at a specific site location for distributed ruptures (P_{2d}). For the relationship between earthquake magnitude and mean displacement of the principal fault, as well as the variability and probability distribution of the variation, we also followed the conventions of these models. Note that a sensitivity analysis has confirmed that the fault displacement hazard remains virtually unchanged even when P_{1p} = 0.01. Details of this analysis were provided in a previous study[12].

The logic tree for the FDPEs based on distance from the earthquake source faults consists of the probability of surface rupture given a magnitude M (P_{1s}), the conditional probability of surface rupture at a specific site location (P_{2s}), and the conditional probability of exceedance on the surface ruptures (P_{3d}). Considering that the 2016 Kumamoto earthquake focal region is located at the western extension of the MTLAFZ (Ikeda et al.[23]), we adopted the FDPEs of Nishizaka et al.[16], which were based on the dataset for the area surrounding the 2016 Kumamoto earthquake focal region (Fig. 1). In the part of the area, the outer zone of southwestern Japan has been classified as exhibiting similar seismotectonics to the Ikata site, with a notably low active fault density (Kakimi et al.[24]). For the probability of surface rupture given a magnitude M (P_{1s}), P_{1s} = 1 because surface ruptures will always occur for characteristic earthquakes, regardless of activity on the geological boundary at shallow depths. The value of P_{2s} at a site away from the earthquake source fault is the conditional probability of surface rupture during a magnitude M earthquake at the assessment site (three-dimensional shortest distance r_1 from the earthquake source faults, and shortest surface distance r_2 from the mapped, pre-existing active faults). The FDPE based on data from the mountain side (outer zone of southwestern Japan) of the 2016 Kumamoto earthquake was adopted, with its weight set to 1. Here, P_{2s} was calculated using 250 m x 250 m unit cell sizes, similar to the FDPEs based on distance from the principal fault, and then calibrated to the value for 160 m x 160 m. P_{3s} is the conditional probability that the fault displacement will exceed a certain value when surface ruptures occur at the assessment site. The FDPEs of Nishizaka et al.[16] for the 2016 Kumamoto earthquake were adopted, setting branches for FDPEs using (1) the dataset for the non-proximal area (r_2 > 1 km) and (2) all data. This approach accounts for the uncertainty resulting from the limited surface rupture data in the far-field used by Nishizaka et al.[16] for the 2016 Kumamoto earthquake. Considering that the shortest surface distance between the Ikata site and mapped, pre-existing active faults is approximately 6 km, the weight was set to 0.7:0.3. Furthermore, the average displacement of the earthquake source faults was calculated from the earthquake magnitude and fault area using the seismic source characterization model[13), 14] in the Ikata SSHAC project. The variability and probability distribution of the variation were assumed to follow the relationship for strike-slip faults (log-normal distribution with a variance of 0.28) provided by Wells and Coppersmith[21].

3. RESULTS AND INTERPRETATION

3.1 Results of fault displacement hazard analysis

The results of the PFDHA are shown in Fig. 6. The annual frequency of a fault displacement occurring directly beneath the critical seismic-resistant facilities at the Ikata site during characteristic earthquakes on the MTLAFZ (Iyo-nada Segment) lies between 1 x 10^{-7} and 1 x 10^{-8} for both the mean and median values, with the mean being larger. For displacements of 0.1 m or greater, the difference between the mean and median increases, and the AEF decreases exponentially with increasing displacement (Fig. 6(a)). Focusing on the AEF for a displacement of 0.01 m, the mean value of 7.0 x 10^{-8} is larger than the median value of 2.8 x 10^{-8}. At this displacement, the 95th percentile is 1.7 x 10^{-7}, the 84th percentile is 1.2 x 10^{-7}, the 16th percentile is 9.7 x 10^{-14}, and the 5th percentile is 8.2 x 10^{-34}. The latter two values are extremely small compared to the median. This result is attributable to the presence of a branch of the BPT distribution yielding an extremely low hazard level, as described below (Section 3.2). A major difference from the previous study[12] is the clear separation in the slopes of the hazard curves between the mean and median in the region of large displacements (> 1 m). To investigate this factor, we decomposed the mean hazard curve by the FDPEs selected at the branch of the conditional probability of exceedance on the surface ruptures. This analysis revealed that, in the large displacement region, the influence of the conventional FDPEs (from Takao et al. (2016)[20] and Petersen et al.[6]), which are based on distance from the principal fault, is dominant (Fig. 6(b)). The hazard curves produced by the new FDPEs of Nishizaka et al.[16] exhibit a steeper slope than the conventional ones, resulting in a more rapid decrease in AEF with increasing displacement. In contrast, the hazard curves from the conventional FDPEs exhibit a gentler slope, maintaining relatively higher AEF values at large displacements. Therefore, the influence of the conventional FDPEs, which maintain a relatively high hazard level in the large displacement range despite their weight of 0.3, became dominant in the mean value. Conversely, the characteristics of the new FDPEs, which were given a weight of 0.7, are reflected in the median value.

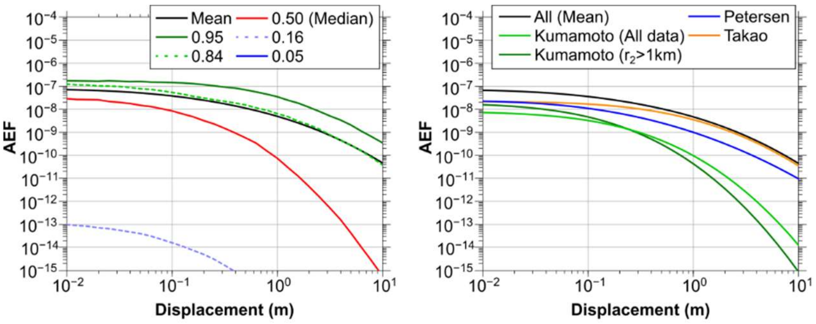

(a) Weighted mean and fractile hazards for all cases

(b) Hazard analysis results separated by the branch for the conditional probability of exceedance on the surface ruptures (Mean)

Fig. 6 Fault displacement hazard analysis results. AEF, annual exceedance frequency. In (a), the 5th percentile is on the order of 10^{-34} and falls outside the display range.

3.2 Results of sensitivity analysis

Figure 7 shows the results of sensitivity analysis for fault displacement hazard at the Ikata site, targeting characteristic earthquakes occurring on the MTLAFZ (Iyo-nada Segment). To illustrate the contribution of each branch item in the logic tree to the fault displacement hazard, a variance contribution plot is shown in Fig. 7(a). This bar graph displays the ratio of the range of the hazard curve for each branch item to the total range of all hazard curves for a specific AEF; a branch item that causes significant changes in the hazard curve as a result of its selection exhibits a higher percentage in the variance contribution plot. We analyzed the contribution of each branch item to the fault displacement hazard at an AEF of 1 x 10^{-8}, which captures the total range of all hazard curves within a specified fault displacement range (0.01–10 m), including those based on conventional FDPEs exhibiting a gentle slope with increasing displacement. Items related to earthquake location and geometry contributed approximately 17%, items related to earthquake magnitude contributed approximately 5%, and items related to earthquake probability of occurrence contributed approximately 59%. These three items, which are related to the seismic source characterization model, accounted for approximately 81% of the total contributions; items related to the fault displacement characterization model accounted for the remaining ca. 19%. In a previous study, the variance contribution plot based on seismic hazard at the Ikata site using the same seismic source characterization model (Iyo-nada Segment) indicated that, for seismic hazard, the contribution of items related to the seismic source characterization model ranged from approximately 67% to 46% (corresponding to AEF values of 1 x 10^{-4} to 1 x 10^{-6})[13]. Thus, the contribution of items related to the seismic source characterization model (especially the earthquake probability of occurrence) at the Ikata site is greater for the fault displacement hazard than for the seismic hazard, and the contribution of items related to the fault displacement characterization model is relatively small.

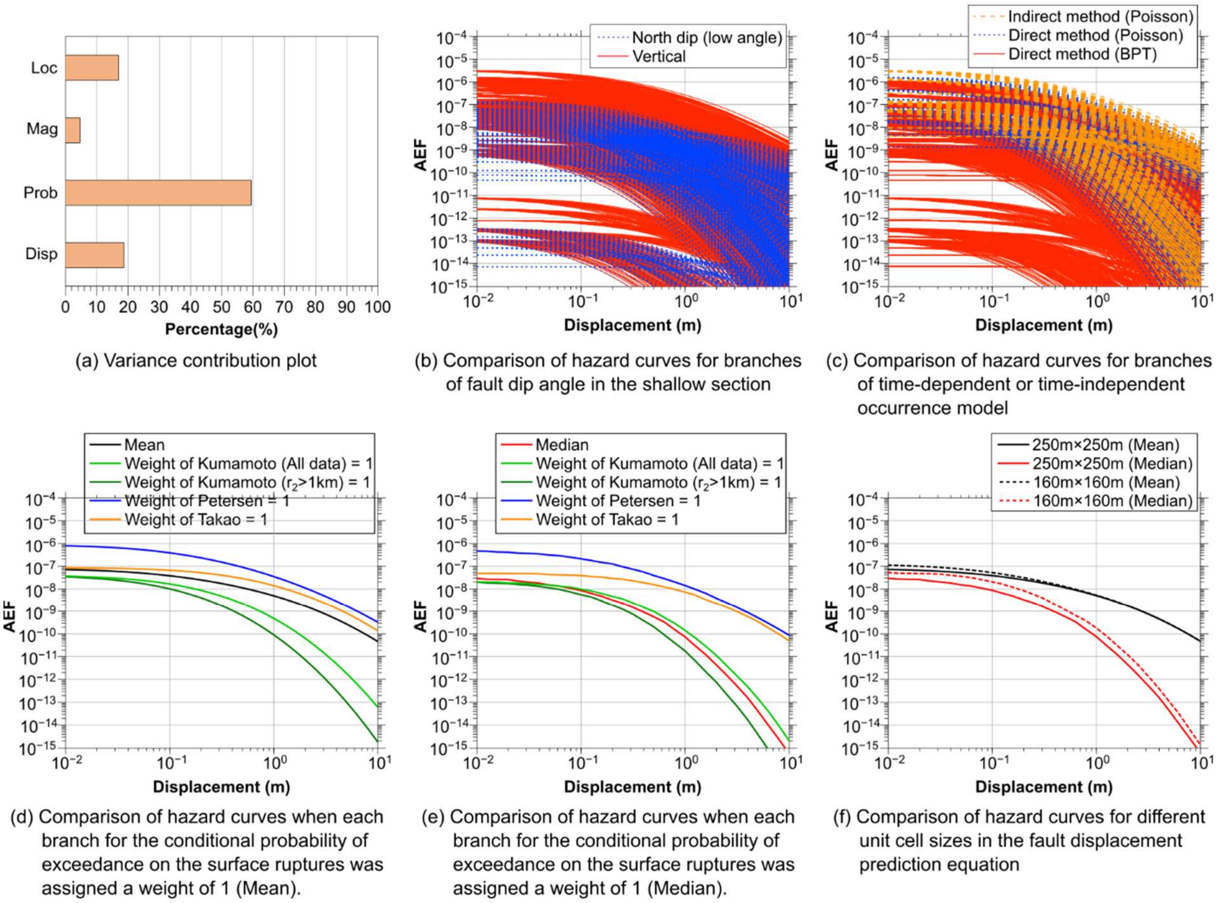

(a) Variance contribution plot

(b) Comparison of hazard curves for branches of fault dip angle in the shallow section

(c) Comparison of hazard curves for branches of time-dependent or time-independent occurrence model

(d) Comparison of hazard curves when each branch for the conditional probability of exceedance on the surface ruptures was assigned a weight of 1 (Mean).

(e) Comparison of hazard curves when each branch for the conditional probability of exceedance on the surface ruptures was assigned a weight of 1 (Median).

(f) Comparison of hazard curves for different unit cell sizes in the fault displacement prediction equation

Fig. 7 Sensitivity analysis results. AEF, annual exceedance frequency. (a) Abbreviations: Loc, earthquake location and geometry; Mag, earthquake magnitude; Prob, earthquake probability of occurrence; Disp, fault displacement characterization model. (f) Comparison of hazard curves based on the regression coefficient of P_{2s} calculated using 160 m x 160 m unit cell sizes based on surface rupture data derived from the 2016 Kumamoto earthquake with the original hazard curve (250 m x 250 m unit cell sizes).

Figures 7(b) and 7(c) show a comparison of hazard curves for all branches of the logic tree, color-coded by fault dip angle in the shallow section and by branch items in the time-dependent or time-independent occurrence model. The branches of fault dip angle in the shallow section are the Vertical (90°) and the North dip (low angle) branch. In the branch adopting the conventional FDPEs based on distance from the principal fault, the shortest distance from the principal fault and the probability of principal rupture given a magnitude M (P_{1p}) are approximately 8 km and 1, respectively, for the Vertical (90°) branch, whereas for the North dip (low angle) branch, they are approximately 600 m and 0.001. Consequently, the hazard curve for the Vertical (90°) branch, which has a greater distance from the principal fault but a higher probability of principal rupture, is significantly larger. This difference is interpreted as the main factor influencing the ~17% share of the contribution from items related to the earthquake location and geometry. The branches of the time-dependent or time-independent occurrence model are the BPT distribution and Poisson process for the direct method, and the Poisson process for the indirect method. The mean recurrence interval is shorter for the indirect method (1000 years) than for the direct method (3060 years), and the branches of the BPT distribution include the three latest faulting events, which took place in AD 1596, 1460 years ago, and 2500 years ago[13), 14)]. This difference in the latest faulting events was interpreted as the main factor contributing to the approximately 59% share of the contribution from the items related to earthquake probability of occurrence. Although the hazard curves for the branches of the Poisson process are concentrated at high levels, the hazard curves for the branches of the BPT distribution exhibit broad variation from high to extremely low levels (Fig. 7(c)).

We assessed the influence of the different FDPEs on the results by examining the mean and median values of the fault displacement hazard when the weight of each FDPE selected at the branch for the conditional probability that the fault displacement will exceed a certain value (P_{3d} or P_{3s}) was changed to 1 (Figs. 7(d), (e)). When the weight for the branch selecting the FDPE of Takao et al. (2016)[20] is changed to 1, the AEF at a displacement of 0.01 m lies between 1 x 10^{-7} and 1 x 10^{-8}, which is only slightly higher than the original hazard. However, for displacements of 0.1 m or greater, the AEF decreases with increasing displacement at a gentler slope than the original hazard curve, resulting in a higher hazard level. The difference is particularly pronounced for the median values (Fig. 7(e)). When the weight of the branch selecting the FDPE of Petersen et al.[6] is changed to 1, the AEF at a displacement of 0.01 m lies between 1 x 10^{-6} and 1 x 10^{-7}, which represents a hazard of a level one order of magnitude higher than the original. For displacements of 0.1 m or greater, the AEF decreases with increasing displacement at a slightly steeper slope than that for the FDPE of Takao et al. (2016)[20], and the two curves converge at high displacement values. When the weight of the branch selecting the FDPE[16] for the non-proximal area relative to mapped active faults around the 2016 Kumamoto earthquake focal region is changed to 1, the AEF at a displacement of 0.01 m lies between 1 x 10^{-7} and 1 x 10^{-8}, which is slightly lower than the original hazard. For displacements of 0.1 m or greater, the AEF decreases with increasing displacement at a steeper slope than the original hazard curve, leading to a greater divergence from it. When the weight of the branch selecting the FDPE[16] derived from all data of the 2016 Kumamoto earthquake is changed to 1, the AEF at a displacement of 0.01 m is equivalent to that of the FDPE[16] for the non-proximal area relative to mapped active faults around the 2016 Kumamoto earthquake focal region. For displacements of 0.1 m or greater, the AEF decreases with increasing displacement at a slightly gentler slope than that for the non-proximal area. For these four hazard curves, the AEF at a displacement of 0.01 m corresponds to the characteristics of the conditional probability of surface rupture at a specific site location (P_{2d} or P_{2s}), whereas the slope associated with increasing displacement corresponds to the characteristics of the conditional probability that the fault displacement will exceed a certain value (P_{3d} or P_{3s}). When applying new FDPEs based on distance from the earthquake source faults[16] to the PFDHA at the Ikata site, the FDPE characteristics result in a slightly lower AEF at a displacement of 0.01 m compared to the conventional FDPEs, and the AEF curves exhibit a steeper slope with increasing displacement than those from conventional FDPEs, thereby reducing the AEF at larger displacements. It is noteworthy that even though these new FDPEs with different characteristics from the conventional ones were incorporated into the logic tree and epistemic uncertainties were considered, the contribution of items related to the fault displacement characterization model remained at only about 19%. Although the need to enhance FDPEs in future work is self-evident, this result underscores the importance of constructing a highly reliable seismic source characterization model (in particular, the earthquake probability of occurrence) in PFDHA.

New FDPEs[16] based on individual surface rupture data derived from the 2016 Kumamoto earthquake are considered to have issues regarding the stability of the regression equation for the conditional probability of surface rupture at a specific site location (P_{2s}) and the calibration by an area ratio, both due to the limited amount of data. Therefore, using the same dataset and methodology as Nishizaka et al.[16], regression coefficients were calculated using 160 m x 160 m unit cell sizes, eliminating the need for calibration by an area ratio ($c_1 = -1.34$, $c_2 = -2.61$, $c_3 = 1.19$, $c_4 = -0.876$, $c_5 = 0.00475$). As a sensitivity analysis, the fault displacement hazards at the Ikata site were calculated based on these coefficients. The mean and median AEF values for a displacement of 0.01 m are 1.1 x 10^{-7} and 5.1 x 10^{-8}, respectively; these values are slightly higher than those for the original hazard (Fig. 7(f)). Because the new FDPEs[16] use the shortest distance from mapped, pre-existing active faults, and considering the mapping accuracy of active fault locations, regression equations using small unit cell sizes can become unstable; therefore, use of FDPEs with moderately larger unit cell sizes is recommended.

4. INSIGHTS GAINED FROM PRACTICE AT THE IKATA SITE

This study incorporated newly proposed FDPEs[16] into the logic tree to update the previously reported PFDHA at the Ikata site[12]. Incorporation of new FDPEs enabled calculation of the fault displacement hazard without using the distance from the principal fault, for which epistemic uncertainties are problematic in classifying surface ruptures, when selecting the branch of the FDPEs based on distance from the earthquake source faults. Here, drawing on experience at the Ikata site, we examine the progress made in addressing the challenges identified in a previous study[12]: (i) expanding surface rupture data to far-field areas; (ii) developing FDPEs that can account for the presence or absence of pre-existing active faults; and (iii) establishing a methodology that can consider site-specific seismotectonics.

Regarding the expansion of surface rupture data to far-field areas, the branch of the FDPEs based on distance from the principal fault includes the FDPE of Takao et al.[19), 20] as the only FDPE for strike-slip faults applicable to the far-field. Therefore, as previously reported[12], we accounted for epistemic uncertainties by setting a branch for the FDPE of Petersen et al.[6], which is applicable up to 2 km from the principal fault. As previously reported[12], the applicability of the FDPE of Takao et al.[19), 20] to the far-field is questionable, because it uses observational data prior to the 2008 Iwate–Miyagi earthquake, leading to significant discrepancies with the conditional probability of surface rupture at a specific site location derived from the 2016 Kumamoto earthquake observational data. The problem of extrapolation beyond the applicability range of such FDPEs and the large differences in the conditional probabilities of surface rupture between FDPEs has also been recognized in the case studies of PFDHA by the IAEA (Valentini et al.[25]). In contrast, the branch of the FDPEs based on distance from the earthquake source faults added in this study employed FDPEs[16] developed for application to far-field areas from the earthquake source faults. These FDPEs utilize surface rupture data[17] derived from the 2016 Kumamoto earthquake, for which a detailed distribution of surface ruptures over a wide area was obtained through a combination of remote sensing techniques and field surveys. Consequently, we expanded the surface rupture data to the far-field and assessed the fault displacement hazard at the Ikata site. The PFDHA results in this study can be considered to have alleviated concerns about insufficient surface rupture data in the far-field, particularly regarding the conditional probability of surface rupture. However, it should be noted that these FDPEs are based on the individual dataset of the 2016 Kumamoto earthquake, raising issues regarding the stability of the regression equation and its applicability to future predictions. Furthermore, regarding the amount of fault displacement, the current FDPEs have been pointed out to lack sufficient far-field data[16]. Further expansion of fault displacement data and improvement of the accuracy of FDPEs should be carried out in the future.

Regarding the development of FDPEs that can account for the presence or absence of pre-existing active faults, neither the FDPEs of Takao et al.[19), 20] nor those of Petersen et al.[6], which were adopted for the branch in the FDPEs based on distance from the principal fault, meet this requirement. Specifically, the latter excluded datasets for far-field surface ruptures, arguing that their characteristics differ from those of typical distributed ruptures, and proposed FDPEs applicable only within 2 km of the principal fault. Recently, new FDPEs of Visini et al.[11] have been proposed that can account for the reactivation of pre-existing faults directly beneath or near the site by using ranked surface rupture data for dip-slip faults (normal and reverse faults); however, no FDPE for strike-slip faults was put forward. During site selection of critical facilities, the applicability of FDPEs for strike-slip faults has been questioned because conventional FDPEs do not sufficiently consider far-field fault displacement. Consequently, the need to consider the reactivation of pre-existing faults far from the principal fault has been pointed out again for strike-slip faults (Ferrario et al.[26]). In the present study, the newly added branch for the FDPEs based on distance from the earthquake source faults employed FDPEs[16] designed to account for the distance from mapped, pre-existing active faults. These FDPEs incorporate the fact that the conditional probability of surface rupture and the conditional probability of exceedance on the surface ruptures are significantly larger near mapped, pre-existing active faults. This approach produced a fault displacement hazard that incorporates the characteristics of the Ikata site, where detailed investigations have confirmed the absence of active faults in the vicinity. However, as discussed in the previous study[12], sites for safety-critical facilities are chosen so as to avoid locations with any potential fault displacement; at these sites, the absence of potential fault displacement is confirmed through thorough investigations, including bedrock excavation. It should be noted that, even with the adoption of new FDPEs that consider the presence of pre-existing active faults mapped through geomorphological investigations, the present hazard does not account for this aspect.

Furthermore, Nishizaka et al.[16] discussed the effects of both static stress changes[27), 28] and dynamic stress changes[29), 30] on the triggering of fault displacements on pre-existing active faults. Their discussion of static stress changes focused on the possibility that fault displacements on pre-existing faults, oriented so as to be favorably reactivated by a static stress change, are triggered by changes in the surrounding stress field induced by slip on the earthquake source faults. To incorporate static stress changes as a correction term in FDPEs, it will be necessary to quantitatively evaluate the relationship between static stress changes and fault displacement through analysis of observational data. Their discussion of dynamic stress changes addressed the potential for such changes accompanying seismic wave passage to trigger displacements on pre-existing faults. At the Ikata site, vertical-array seismic observations down to the seismological bedrock at a depth of 2000 m revealed a unique site response with almost no amplification from the top of the seismological bedrock to the surface, and even attenuation in the frequency range above 1 Hz (Nishizaka et al.[31]). Although there have been few reports on the influence of ground motion on fault displacement, it has been pointed out that resonance occurring at frequencies close to the low-order natural frequencies of the bedrock may promote fault displacements at the surface (Haba et al.[32]). It is therefore necessary to develop risk assessment methods that superimpose ground motions and fault displacements[33)–35]. In the future, the relationship between near-surface ground motions and fault displacements should be examined through combined analyses of observational data and analytical studies. Thus, the effects of static and dynamic stress changes on fault displacement remain an area that requires further investigation. Studies based on distance from the earthquake source faults are expected to be useful in promoting a better understanding of the physical background.

Regarding the establishment of a methodology that can consider site-specific seismotectonics, the FDPEs of both Takao et al.[19), 20] and Petersen et al.[6], adopted for the branch in the FDPEs based on distance from the principal fault, are ergodic equations formulated from observational data derived from numerous earthquakes occurring in various regions. Thus, they are not capable of considering site-specific seismotectonics. In contrast, the branch of the FDPEs based on distance from the earthquake source faults added in this study adopted FDPEs of Nishizaka et al.[16] formulated from observational data of surface ruptures associated with the 2016 Kumamoto earthquake in the outer zone of southwestern Japan, which shares common seismotectonics with the Ikata site. This approach yielded a fault displacement hazard that incorporates the characteristics of the outer zone of southwestern Japan[24], a seismotectonic province in which the active fault density is considered to be extremely low relative to other parts of the same country. However, with regard to the amount of fault displacement, the regression equation[16] was formulated from a dataset combined with observations from the Beppu–Shimabara Rift Zone (plains side) because the data from the outer zone of southwestern Japan (mountainous side) were insufficient. Furthermore, the effect of variation in bedrock geology within the same outer zone of southwestern Japan should be considered. Expansion of the dataset in future studies is therefore desirable.

A review (Valentini et al.[36]) summarizing the approximately 25 years since PFDHA was proposed as a methodology suggested three main directions for future enhancement of FDPEs: first, enriching existing fault displacement databases with high-quality observations and measurements; second, adopting physics-based models to bridge gaps in empirical data and improve predictive capabilities; and third, refining existing modeling approaches. The findings from the practice at the Ikata site, which demonstrate the characteristics of new FDPEs based on high-quality observations and measurements from recent earthquakes, also support the importance of enhancing available FDPEs in line with their suggestions. Moving forward, it is anticipated that the development of versatile and reliable FDPEs will progress through two parallel approaches: (i) expanding fault displacement data to include regions with different seismotectonics and (ii) developing physics-based models that relate the characteristics of surface ruptures to earthquake source faults.

5. CONCLUSIONS

This study applied newly proposed FDPEs based on distance from strike-slip earthquake source faults to the Ikata site, considering challenges identified during the first full-scale implementation of PFDHA in Japan at the Ikata site. The characteristics of the new FDPEs and the insights gained from the practice at the Ikata site were examined. The results of PFDHA indicate that the annual frequency of fault displacements occurring directly beneath the critical seismic-resistant facilities at the Ikata site during characteristic earthquakes on the MTLAFZ (Iyo-nada Segment) lies between 1 x 10^{-7} and 1 x 10^{-8}. For displacements of 0.1 m or greater, the AEF decreases exponentially with increasing displacement. Sensitivity analysis results suggested that the contribution of items related to the seismic source characterization model (especially the earthquake probability of occurrence) is greater in the fault displacement hazard at the Ikata site, whereas the contribution of items related to the fault displacement characterization model is relatively small. When applying the new FDPEs to the PFDHA at the Ikata site, their characteristics result in a slightly lower AEF at a displacement of 0.01 m compared to the conventional FDPEs, and they exhibit a steeper slope with increasing displacement than the conventional FDPEs. Fault displacement hazard can be calculated without using the distance from the principal fault, for which epistemic uncertainties are problematic in classifying surface ruptures, when selecting the branch of the FDPEs based on distance from the earthquake source faults. Steady progress was achieved in addressing the challenges identified in the previous study: (i) expanding surface rupture data to far-field areas; (ii) developing FDPEs that can account for the presence or absence of pre-existing active faults; and (iii) establishing a methodology that can consider site-specific seismotectonics. This study describes the characteristics of the newly proposed FDPEs and demonstrates their practicality and the effectiveness of the approach. The insights gained from the practice at the Ikata site are useful for enhancing the versatility and reliability of FDPEs and are expected to markedly contribute to the future development of PFDHA.

ACKNOWLEDGMENT

We used the seismic source characterization model developed by the team of experts evaluating seismic source characteristics in cooperation with many other contributors under the Ikata SSHAC Project. We thank Kensuke Arai of Ohsaki Research Institute for his essential assistance with PFDHA, and Kazuya Yamamoto of Hanshin Consultants Co. for his contributions to the calculations of the regression equations used in the sensitivity analysis.

REFERENCES

1) Youngs, R. R., Arabasz, W. J., Anderson, R. E., Ramelli, A. R., Ake, J. P., Slemmons, D. B., McCalpin, J. P., Doser, D. I., Fridrich, C. J., Swan III, F. H., Rogers, A. M., Yount, J. C., Anderson, L. W., Smith, K. D., Bruhn, R. L., Knuepfer, P. L. K., Smith, R. B., dePolo, C. M., O'Leary, D. W., Coppersmith, K. J., Pezzopane, S. K., Schwartz, D. P., Whitney, J. W., Olig, S. S. and Toro, G. R.: A Methodology for Probabilistic Fault Displacement Hazard Analysis (PFDHA), *Earthquake Spectra*, Vol. 19, No. 1, pp. 191–219, 2003.
2) International Atomic Energy Agency: Seismic Hazards in Site Evaluation for Nuclear Installations, Specific Safety Guide, No. SSG-9 (Rev. 1), 78 pp., 2022.
3) Valentini, A., Fukushima, Y., Contri, P., Ono, M., Sakai, T., Thompson, S. C., Viallet, E., Annaka, T., Chen, R., Moss, R. E. S., Petersen, M. D., Visini, F. and Youngs, R. R.: Probabilistic Fault Displacement Hazard Assessment (PFDHA) for Nuclear Installations According to IAEA Safety Standards, *Bulletin of the Seismological Society of America*, Vol. 111, No. 5, pp. 2661–2672, 2021.
4) Testa, A., Boncio, P., Pace, B., Mirabella, F., Pauselli, C., Ercoli, M., Auciello, E., Visini, F. and Baize, S.: Probabilistic Fault Displacement Hazard Analysis in an Extensional Setting: Application to a Strategic Dam and Methodological Implications, *Engineering Geology*, Vol. 343, 107817, pp.

1–13, 2024.

5) Cagnan, Z.: Comparison of Probabilistic Fault Displacement Hazard Assessment Results with Observed Permanent Ground Displacements in the Aftermath of the 6 February 2023 Türkiye Earthquakes, *Bulletin of the Seismological Society of America*, Vol. 115, No. 4, pp. 1891–1906, 2025.
6) Petersen, M. D., Dawson, T. E., Chen, R., Cao, T., Wills, C. J., Schwartz, D. P. and Frankel, A. D.: Fault Displacement Hazard for Strike-Slip Faults, *Bulletin of the Seismological Society of America*, Vol. 101, No. 2, pp. 805–825, 2011.
7) Takao, M., Tsuchiyama, J., Annaka, T. and Kurita, T.: Application of Probabilistic Fault Displacement Hazard Analysis in Japan, *Journal of Japan Association for Earthquake Engineering*, Vol. 13, No. 1, pp. 17–36, 2013 (in Japanese).
8) Nurminen, F., Boncio, P., Visini, F., Pace, B., Valentini, A., Baize, S. and Scotti, O.: Probability of Occurrence and Displacement Regression of Distributed Surface Rupturing for Reverse Earthquakes, *Frontiers in Earth Science*, Vol. 8, 581605, pp. 1–18, 2020.
9) Ferrario, M. F. and Livio, F.: Conditional Probability of Distributed Surface Rupturing during Normal-Faulting Earthquakes, *Solid Earth*, Vol. 12, pp. 1197–1209, 2021.
10) Rodriguez Padilla, A. M. and Oskin, M. E.: Displacement Hazard from Distributed Ruptures in Strike-Slip Earthquakes, *Bulletin of the Seismological Society of America*, Vol. 113, No. 6, pp. 2730–2745, 2023.
11) Visini, F., Boncio, P., Valentini, A., Scotti, O., Nurminen, F., Baize, S. and Pace, B.: Empirical Regressions for Distributed Faulting of Dip-Slip Earthquakes, *Earthquake Spectra*, Vol. 41, No. 4, pp. 2968–3001, 2025.
12) Nishizaka, N., Onishi, K., Ishikawa, Y., Ono, M., Miyakoshi, J., Ikeda, M., Tsuji, T., Kumamoto, T. and Okumura, K.: Probabilistic Fault Displacement Hazard Analysis Using Model of Seismic Source Characteristics at the Ikata Site Based on Guidelines for SSHAC Level 3, *Journal of Japan Association for Earthquake Engineering*, Vol. 24, No. 2, pp. 57–78, 2024.
13) Kumamoto, T., Okumura, K., Tsukuda, E., Tsusumi, H., Tsutsumi, H., Toda, S., Tokuyama, H., Onishi, K., Nishizaka, N., Ohno, Y., Sakai, T. and Kameda, H.: Development of Model of Seismic Source Characteristics at the Ikata Site Based on Guidelines for SSHAC Level 3, *Journal of Japan Association for Earthquake Engineering*, Vol. 24, No. 2, pp. 30–56, 2024.
14) Kameda, H., Kumamoto, T., Fujiwara, H., Okumura, K., Tsukuda, E., Tsutsumi, H., Tsutsumi, H., Toda, S., Tokuyama, H., Ebisawa, K., Kagawa, T., Si, H., Furumura, T., Miyake, H., Morikawa, N., Okumura, T. and Miyakoshi, J.: Ikata SSHAC Project Final Report, 2020 (in Japanese). https://www.yonden.co.jp/energy/atom/safety/sshac_project/index.html (last accessed on March 1, 2026)
15) Kusumoto, S.: Dip Distribution of Oita–Kumamoto Tectonic Line Located in Central Kyushu, Japan, Estimated by Eigenvectors of Gravity Gradient Tensor, *Earth, Planets and Space*, Vol. 68, 153, pp. 1–8, 2016.
16) Nishizaka, N, Onishi, K., Ikeda, M., Si, H., Yamamoto, K. and Tsuji, T.: Characteristics of Far-Field Surface Ruptures Caused by Two Recent Strike-Slip Earthquakes: Insights into Fault Displacement Prediction, *Seismological Research Letters*, Vol. 97, No. 4, pp. 2631–2646, 2026.
17) Nurminen, F., Baize, S., Boncio, P., Blumetti, A. M., Cinti, F. R., Civico, R. and Guerrieri, L.: SURE 2.0—New Release of the Worldwide Database of Surface Ruptures for Fault Displacement Hazard Analyses, *Scientific Data*, Vol. 9, 729, pp. 1–18, 2022.
18) Takahashi, K., Ikeda, M., Sato, T., Adachi, K., Nishizaka, N., Onishi, K., Ohno, Y., Tsuyuguchi, K. and Tsuji, T.: Distribution and Activity of Median Tectonic Line in the Iyo-Nada Sea off Northwestern Shikoku Based on Seismic Survey, *Active Fault Research*, Vol. 53, pp. 13–32, 2020 (in Japanese).
19) Takao, M., Ueta, K., Annaka, T., Kurita, T., Nakase, H., Kyoya, T. and Kato, J.: Reliability Improvement of Probabilistic Fault Displacement Hazard Analysis, *Journal of Japan Association for Earthquake Engineering*, Vol. 14, No. 2, pp. 16–36, 2014 (in Japanese).
20) Takao, M., Tani, T., Oshima, T., Annaka, T. and Kurita, T.: Maximum Likelihood Estimation of the Parameters Regarding Displacement Evaluation of Distributed Fault in PFDHA, *Journal of*

Japan Association for Earthquake Engineering, Vol. 16, No. 2, pp. 96–101, 2016 (in Japanese).
21) Wells, D. L. and Coppersmith, K. J.: New Empirical Relationships among Magnitude, Rupture Length, Rupture Width, Rupture Area, and Surface Displacement, *Bulletin of the Seismological Society of America*, Vol. 84, No. 4, pp. 974–1002, 1994.
22) U.S. Nuclear Regulatory Commission: Confirmatory Analysis of Seismic Hazard at the Diablo Canyon Power Plant from the Shoreline Fault Zone, Research Information Letter 12-01, pp. C1–C23, 2012. https://www.nrc.gov/docs/ML1212/ML121230035.pdf (last accessed on March 1, 2026)
23) Ikeda, M., Toda, S., Kobayashi, S., Ohno, Y., Nishizaka, N. and Ohno, I.: Tectonic Model and Fault Segmentation of the Median Tectonic Line Active Fault System on Shikoku, Japan, *Tectonics*, Vol. 28, TC5006, pp. 1–22, 2009.
24) Kakimi, T., Matsuda, T., Aida, I. and Kinugasa, Y.: A Seismotectonic Province Map in and around the Japanese Islands, *Zisin 2nd ser.*, Vol. 55, pp. 389–406, 2003 (in Japanese).
25) Valentini, A., Fukushima, Y., Contri, P. and Gülerce, Z.: The IAEA Exercise on Probabilistic Fault Displacement Hazard Assessment, *Earthquake Spectra*, Vol. 41, No. 4, pp. 3002–3021, 2025.
26) Ferrario, M. F., Livio, F. and Serva, L.: Prediction of Coseismic Rupture Locations from Fault Maps, *Bulletin of the Seismological Society of America*, Vol. 115, No. 4, pp. 1551–1569, 2025.
27) Goto, H., Tsutsumi, H., Toda, S. and Kumahara, Y.: Geomorphic Features of Surface Ruptures Associated with the 2016 Kumamoto Earthquake in and around the Downtown of Kumamoto City, and Implications on Triggered Slip along Active Faults, *Earth, Planets and Space*, Vol. 69, 26, pp. 1–12, 2017.
28) Takahashi, N., Uchida, H., Ikeda, M. and Toda, S.: An Overview of the 2019 Ridgecrest, California, Earthquake Sequence and a Recent Trend in Post-Earthquake Survey, *Active Fault Research*, Vol. 53, pp. 51–65, 2020 (in Japanese).
29) Toda, S. and Ishimura, D.: Evaluation of Short Active Faults Reflected from Distributed Minor Surface Breaks Found at Recent Inland Large Earthquakes Including the 2016 Kumamoto Earthquake, *The Quaternary Research*, Vol. 58, pp. 121–136, 2019 (in Japanese).
30) Fujiwara, S., Nakano, T. and Morishita, Y.: Detection of Triggered Shallow Slips Caused by Large Earthquakes Using L-Band SAR Interferometry, *Earth, Planets and Space*, Vol. 72, 119, pp. 1–23, 2020.
31) Nishizaka, N., Sato, H., Tsuji, T., Ishikawa, Y., Nagai, C. and Yamauchi, Y.: Characteristics and Controlling Factors of Seismic Site Response at a Crystalline Bedrock Site Based on Quality Factor Inversion Using Deep Borehole Data, Scientific Reports, Vol. 15, 13230, pp. 1–16, 2025.
32) Haba, K., Sawada, M., Watanabe, K. and Hori, M.: A Fundamental Study on the Effect of Seismic Motion on Surface Fault Displacement, *Proceedings of the 65th National Congress of Theoretical and Applied Mechanics*, OS10-02-03, 2019 (in Japanese).
33) Gürpinar, A., Serva, L., Livio, F. and Rizzo, P. C.: Earthquake-Induced Crustal Deformation and Consequences for Fault Displacement Hazard Analysis of Nuclear Power Plants, *Nuclear Engineering and Design*, Vol. 311, pp. 69–85, 2017.
34) Atomic Energy Society of Japan: A Standard for Procedure of Fault Displacement Probabilistic Risk Assessment for Nuclear Power Plants: 2021 (AESJ-SC-RK009:2021), 306 pp., 2021 (in Japanese).
35) Sawada, M., Haba, K. and Hori, M.: Predictive Simulation for Surface Fault Occurrence Using High-Performance Computing, *GeoHazards*, Vol. 3, pp. 88–105, 2022.
36) Valentini, A., Visini, F., Boncio, P., Scotti, O. and Baize, S.: Twenty-Five Years of Probabilistic Fault Displacement Hazard Assessment, *Reviews of Geophysics*, Vol. 63, e2024RG000875, pp. 1–35, 2025.

(Original Japanese Paper Published: May, 2026)
(English Version Submitted: May 29, 2026)
(English Version Accepted: July 6, 2026)